BBAA VI International Colloquium on:
Bluff Bodies Aerodynamics & Applications
Milano, Italy, July, 20-24 2008

OPEN CHANNEL FLOW OVER A PAIR OF RECTANGULAR CYLINDERS AT INCIDENCE

J. M. Tsitaka[1], M. Agelinchaab[1], M. F. Tachie[1], and C. Katopodis[2]

[1]University of Manitoba
Winnipeg, Manitoba, R3T 5V6, Canada
e-mail: tachiemf@cc.umanitoba.ca

[2] Fisheries and Oceans Canada
Winnipeg, Manitoba, R3T 2N6, Canada
e-mails: Chris.Katopodis@dfo-mpo.gc.ca

Keywords: Open channel flow, Turbulent wake, Rectangular cylinders, Angle of incidence

Abstract. *This paper reports detailed velocity measurements conducted in turbulent wakes generated by a pair of rectangular cylinders inclined at four different angles of incidence relative to the approach open channel flow. The length to thickness ratio of the cylinder was 8.3. The cylinder pair was mounted vertically on the floor of the open channel, and the center-to-center spacing between the cylinder pair was kept constant at 51 mm. For each of the four cylinder inclinations (0^o, 7.5^o, 15^o and 22.5^o), a high resolution particle image velocimetry technique was used to conduct detailed measurements in the streamwise-spanwise plane. From these measurements, iso-contours and profiles of the mean velocity, turbulent intensities and Reynolds shear stress were obtained to document some of the salient features of open channel turbulent wakes generated by a pair of rectangular cylinders at various angles of incidence.*

1 INTRODUCTION

Fluid flows around cylinders are encountered in diverse engineering applications including flow around tall buildings, bridges, offshore rigs, trashracks for hydraulic turbines, cooling towers and heat exchangers. For these reasons, numerous studies have been conducted to understand the characteristics of turbulent wake generated by circular and rectangular cylinders. Excellent reviews of fluid flows around rectangular cylinders can be found in Matsumoto [1] and Knisley [2]. The vast majority of prior experimental studies were conducted around single rectangular cylinders at zero angle of incidence [3, 4]. For example, Nakagawa et al [3] studied the near-wake region of rectangular cylinders of varying aspect ratio (i.e. ratio of the cylinder length in the flow direction, L, to its thickness, D) in a channel flow. The aspect ratio was varied from L/D = 0.5 to 3, and a laser Doppler velocimetry (LDV) was used to conduct the velocity measurements. It was observed that, for each cylinder configuration, the flow separated close to the leading. However, the subsequent evolution of the wake flow depends strongly on L/D. The characteristics of turbulent wake of a rectangular cylinder (with L/D = 9) in an open channel were studied by Agelinchaab et al [4]. Velocity measurements were made using particle image velocimetry (PIV) technique to investigate the effects of the free water surface and plane solid wall on the structure and evolution of the wake. A number of wind tunnel studies have also been conducted to understand the characteristics of turbulent flow past rectangular cylinders at different inclinations [1, 5]. Matsumoto et al [1] used hotwire and spectral density analyzer to determine vibration amplitudes and Strouhal numbers of a rectangular cylinder with L/D = 2 at various angles of incidence ($0° \leq \delta \leq 90°$). Pal [5] examined the effects of freestream turbulence levels (0.40, 5.23 and 7.23%) on the characteristics of a turbulent wake developed from the trailing edges of a flat plate. The aspect ratio of the plate was L/D = 62.5 and the measurements were conducted at the following angles of incidence: δ = -3°, 0°, 6°. It was found that the wake centerline velocity recovered faster with increasing freestream turbulence. More recently, Dutta et al [6] used hotwire to document the salient features of the wake downstream of a square cylinder at various angles of incidence ($0° \leq \delta \leq 60°$) to the approach flow. Their results showed that the velocity fluctuations decay in the downstream direction. The slowest decay rate was observed at δ = 45°. Oudhensden et al [7] used a combination of PIV and proper orthogonal decomposition data post-processing techniques to investigate the effect of incidence angles (δ = 0° to 15°) on the coherent structures in the near wake region.

Although, turbulent flows around and downstream of a single cylinder have been studied extensively, the characteristics of flow around a pair of identical rectangular cylinders at incidence to an approach open channel flow have not been studied in detail. Therefore, the goal of the present work is to document some of the salient features of turbulent wake generated by a pair of identical rectangular cylinders at various inclinations to an approach open channel flow. The results will provide a better physical understanding of turbulent flows of engineering importance, and benchmark datasets that will be invaluable for validating numerical modelling.

2 EXPERIMENTAL SET-UP AND MEASUREMENT PROCEDURE

The experiments were performed in a re-circulating open channel having a test section that was 2500 mm long, 200 mm wide and 200 mm deep. A provisional test section made from 6 mm thick acrylic plate was inserted into the main channel to hold the cylinder in place. The insert was 2500 mm long, 184 mm wide and 190 mm deep, and its base was tightly screwed onto the floor of the main channel. The cylinders consist of transparent acrylic plates of nominal thickness, D = 12 mm and length, L = 100 mm. The cylinder height was H = 190 and the centre-to-centre spacing between the cylinders was b = 51 mm. The experiments were performed for the following four angles of incidence relative to the approach flow: δ = 0°, 7.5°, 15.0°, and 22.5°, where δ = 0° refers to when the cylinder was aligned with the approach flow direction. The approach freestream velocity and depth of flow was maintained at U_e =

0.385 m/s and h = 140 mm, respectively. Figure 1 shows a schematic diagram of the top and side views of the inserted test section. It also defines some of the flow nomenclature and the Cartesian coordinates system used. Figure 1b shows sketches of the mean velocity profile of the approach boundary layer as well as profiles upstream, within and downstream of the cylinder pair in the x-z plane. As shown, x, y and z are, respectively, in the streamwise, wall-normal and spanwise directions; x = 0 at the trailing edges of the cylinders, y = 0 at the channel floor, z = 0 at the channel mid-span.

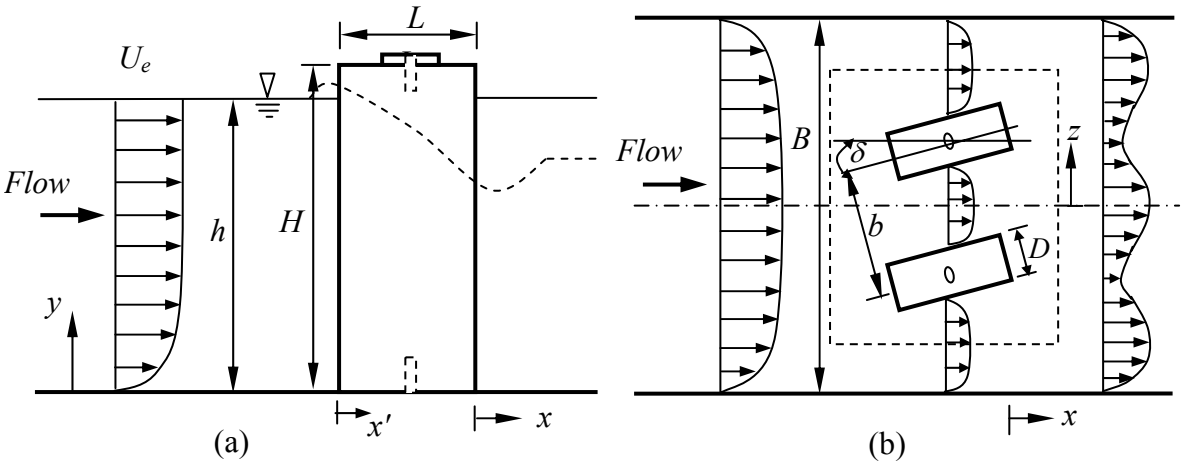

Figure 1: Side (a) and plan (b) views of test section

The PIV technique was used to conduct the velocity measurements. The flow was seeded with 5 μm polyamide seeding particles whose specific gravity was 1.03. An Nd-YAG, 120 mJ/pulse laser of 532 nm wavelength was used to illuminate the flow field. The laser sheet was located at the mid-depth of flow (i.e., at a distance y = 70 mm above the channel floor) and spanned the x-z plane. A 12-bit high-resolution digital camera (Dantec Dynamic HiSense 4M camera) that uses a CCD with 2048 pixels × 2048 pixels and has a 7.4 μm pixel pitch was used to image the flow field. In order to achieve adequate spatial resolution around the cylinders, it was necessary to image the cylinder pair with two different fields of view. The measurements were made at a field of view of 82 mm × 82 mm. The instantaneous images were processed using the adaptive correlation option of FlowManager developed by Dantec Dynamics Inc. A three-point Gaussian curve fit was used to determine particle displacement with sub-pixel accuracy. An interrogation area of 32 × 16 pixels with 50% overlap was employed. This resulted in a spatial resolution of 0.64 mm × 0.32 mm. The particle image diameter was d_p = 2.1 pixels, a value that is very close to the recommended optimum value of $d_p \approx 2$ pixels required to minimize peak locking [8]. In fact, the histograms of the instantaneous images show no evidence of peak locking. The mean velocity and turbulent statistics reported subsequently were calculated using 1500 instantaneous image pairs.

Uncertainty analysis was made following the AIAA standard derived and explained by Coleman and Steele [9]. Detailed analyses of bias and precision errors inherent in the PIV technique are available in Prasad et al [10] and Forliti et al [11]. On the basis of the size of interrogation area and curve fitting algorithm used to calculate the instantaneous vector maps, and the large number of instantaneous images used to calculate the mean velocity and turbulent statistics, the uncertainty in the mean velocities at 95% confidence level was estimated to be ±2%. The uncertainties in turbulent intensities and Reynolds shear stress are estimated to be ±6% and ±10% of the peak values. Close to the rectangular cylinders, uncertainties in mean velocities and Reynolds stress are estimated to be ±2.5% and ±12.5%, respectively.

3 RESULTS AND DISCUSSION

3.1 Flow Qualification

Velocity measurements were obtained at x/D = -35 (i.e., upstream of the cylinders) to characterize the approach open channel flow. As stated earlier, the approach freestream velocity and depth of flow were maintained at U_e = 0.385 m/s and h = 140 mm, respectively. The corresponding Reynolds number based on the approach velocity and depth of flow ($Re_h = U_e h/\nu$) was 53900 while the Froude number ($F = U_e/[gh]^{0.5}$) was 0.33. The approach flow was, therefore, in turbulent and sub-critical regimes. The Reynolds number based on the approach velocity and cylinder thickness ($Re_D = U_e D/\nu$) was 4620.

The mean streamwise velocity distributions and turbulent intensity of the approach flow are shown in Fig. 2. The profiles are as expected for an open channel flow. The background turbulence level close to the free surface was u/U_e = 0.07, which is an order of magnitude higher than typical values reported in wind tunnel experiments. Figure 2c shows the dip in the free surface close to the cylinder pair (relative to the undisturbed free surface). It was observed that the approach flow was substantially distorted by the presence of the cylinder pair, and the degree of distortion increased with inclination. The dips generally increase and extend over wider distance as the cylinder inclination was increased. As noted earlier, arrays of rectangular bars/cylinders are used to construct trashracks that are installed at inlets of hydraulic turbines to prevent debris from entering and damaging the turbine components. They are also used to prevent fish of certain sizes from being entrained into the turbines. From fish perspective, inclined cylinders are desirable because they would reduce the potential of fish entrainment in comparison to aligned cylinders. However, the results presented in Fig. 2c imply that head losses across inclined cylinders would increase with cylinder inclination, an undesirable outcome for hydro companies. This is consistent with higher effective sectional blockage associated with inclined cylinders.

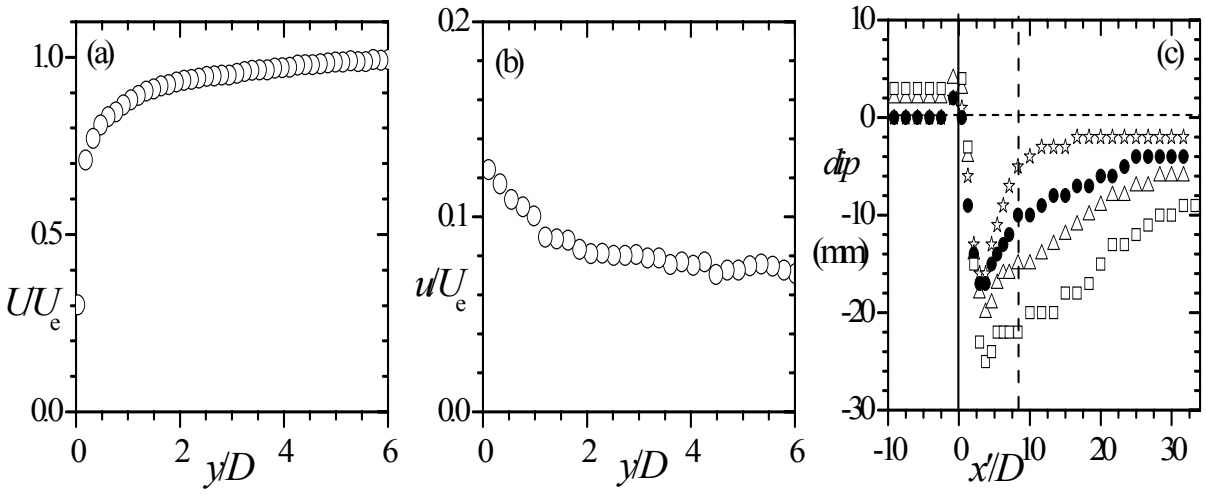

Figure 2: Mean velocity distribution (a), streamwise turbulent intensity (b), and dip in the free surface close to the cylinders, (c). Symbols in (c): δ = 0.0° (☆), 7.5° (●), 15.0° (△), 22.5° (□).

3.2 Mean streamlines and iso-contours of mean velocity and Reynolds shear stress

The iso-contours of dimensionless mean velocity and Reynolds shear stress at δ = 0° to 22.5° are shown in Figs. 3 and 4. The iso-contours were made dimensionless using the approach

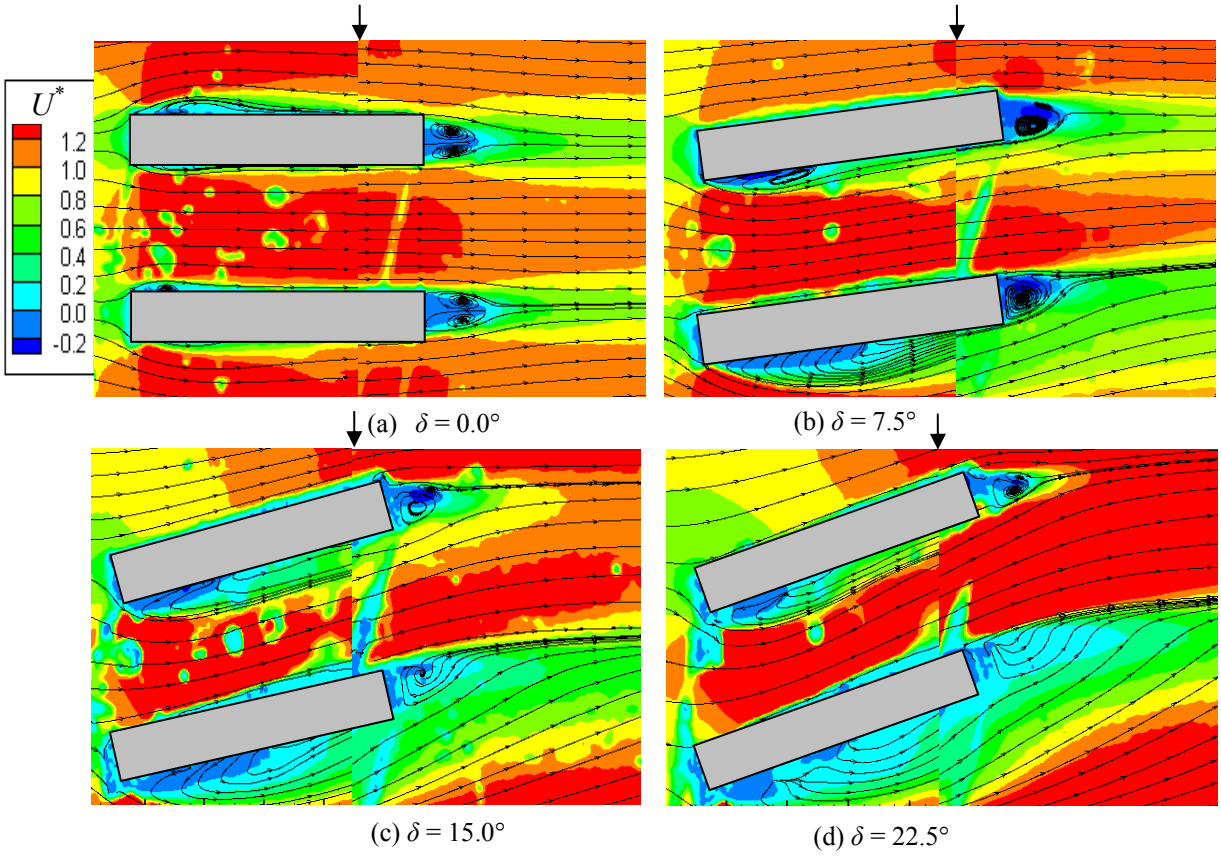

Fig. 3: Iso-contours of mean velocity ($U^* = U/U_e$) for incidence angles of δ = 0.0° (a), 7.5° (b) 15.0° (c) 22.5° (d).

velocity (U_e). The corresponding mean streamlines are superimposed on each plot to reveal the mean flow pattern. As indicated earlier, two adjacent planes were used to image the flow field around the cylinders so as to achieve a high spatial resolution. These two planes are laid side by side in Figs. 3 and 4. An arrow '↓' is used to indicate the point of contact of the two planes. The approximate locations of the cylinders are also shown in the figures. For all test cases, the flow separated near the forward corners of the cylinders; however, the shear layer and vortex formation depend strongly on cylinder inclination. The separated shear layer reattached on either side of the cylinders and produced shallow recirculation zones along the side of each cylinder. This observation is consistent with prior studies that, for single or arrays of rectangular cylinders with $L/D \geq 3$, the separated shear layer would reattach onto the cylinders. It should also be noted that as the cylinder inclination increased, the recirculation bubble on the leeward side of the cylinders increased while that formed at the windward side became less distinct and eventually disappeared. Note that the mean flow pattern between the inclined cylinders is skewed or asymmetric. Due to the higher effective sectional blockage associated with inclined cylinders, the $(U/U_e)_{max}$ between the inclined cylinder pair is significantly increased. Downstream of the aligned cylinders, a pair of well-defined symmetrical counter-rotating vortices is formed at the trailing edge of each cylinder. The size and strength of these vortices are similar. For $\delta > 0°$, the vortices downstream of the cylinders are less distinct and asymmetric. The more asymmetric nature of the flow pattern and recirculation bubbles around the cylinders at incidence would modify the pressure recovery. The implication of this to rectangular shaped structures at incidence is that they would produce asymmetric hydrodynamic loads

that may lead to more severe vibration problems in comparison with aligned rectangular shaped structures.

The iso-contours of dimensionless Reynolds shear stress ($-uw/U_e^2$) are shown in Fig. 4. The plots show higher turbulence levels around the outer edge of the recirculation bubbles formed close to the cylinder leading edge and also within the downstream wake regions. The Reynolds shear stress produced by the inclined cylinders is asymmetric in accordance with the asymmetric mean velocity field observed in Figs. 3b, 3c and 3d. Moreover, the signs of the Reynolds shear stress on opposite sides of the wake axes are also different in accordance to the orientation of the mean shear layer. It is observed that cylinder inclination also increased the magnitude of the Reynolds shear stress substantially in comparison to the measured data for the aligned cylinders.

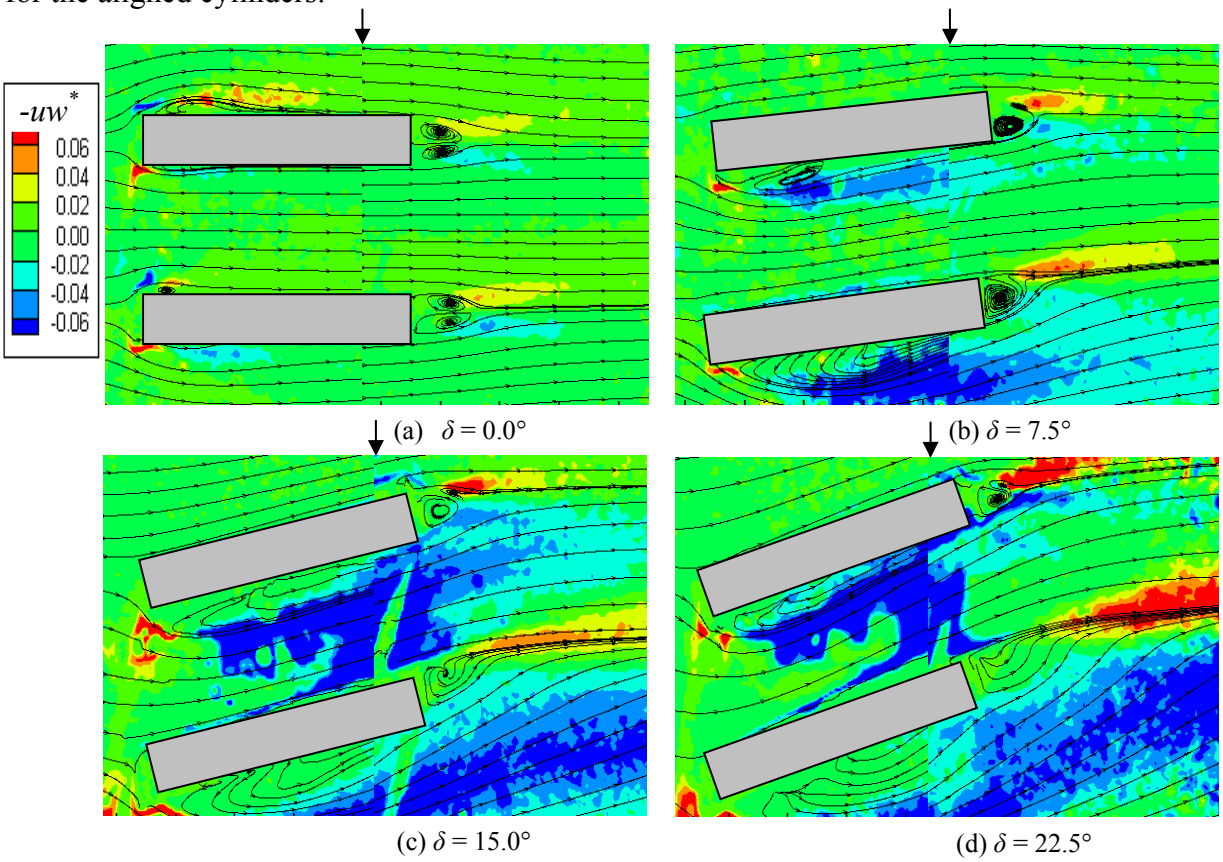

Fig. 4: Iso-contours of Reynolds shear stress ($uw^* = -uw/U_e^2$) for incidence angles of δ = 0.0° (a), 7.5° (b) 15.0° (c) 22.5° (d).

3.3 Mean velocities and turbulence quantities

In this section, the profiles of the mean velocity and turbulent quantities are plotted to validate some of the qualitative observations made in the preceding section. The data are made dimensionless using the approach velocity, U_e. In the plots, appropriate intermediate data points are skipped to decrease data congestion.

3.3.1. Mean velocities and turbulence intensities along the wake

Figure 5 shows the effects of incidence angles on the profiles of the mean velocity and turbulent quantities along the wake centerline of each of the cylinder pair. With reference to Fig. 1b, the cylinder at positive z is denoted as 'top' cylinder and that at negative z is denoted as

'bottom' cylinder in the figure caption for Fig. 5. It should be noted that $x = 0$ is located at the trailing edge of the cylinders. Furthermore, x is made dimensionless using the cylinder thickness (D = 12 mm). At $\delta = 0°$, the recirculation bubble length (l_r) of the top cylinder and the bottom cylinder are similar ($l_r/D \approx 1.50$). Here, l_r is defined as the distance between the trailing edge ($x = 0$) and the x-location where $U/U_e = 0$, downstream of the cylinder. As δ increases, l_r values for both the top and bottom cylinders decrease. However, the l_r value for the bottom cylinder decreases at such a faster rate that at $\delta = 22.5°$, $l_r/D \approx 0.20$. Meanwhile, the l_r/D value for the top cylinder is 1.10. For the aligned cylinder pair ($\delta = 0°$), the recovery of the mean velocity towards its upstream value ($U/U_e = 1$) occurs at the same rate for the top and bottom cylinders, but $(U/U_e)_{max}$ is less than unity. At $\delta = 22.5°$, the values of U/U_e downstream of the top cylinder increases very rapidly, and $(U/U_e)_{max}$ exceeds unity. However, the recovery of the mean velocity for the bottom cylinder is very slow, as a result, $(U/U_e)_{max}$ is less than unity. The variations of the streamwise turbulent intensity and Reynolds shear stress with δ are shown in Figs. 5b and 5, respectively. In general, the peak values increase with δ but the profile downstream of the 'top' cylinder is significantly higher than the corresponding profile downstream of the 'bottom' cylinder. The magnitude of the Reynolds shear stress is relatively higher for inclined cylinders than for aligned cylinders.

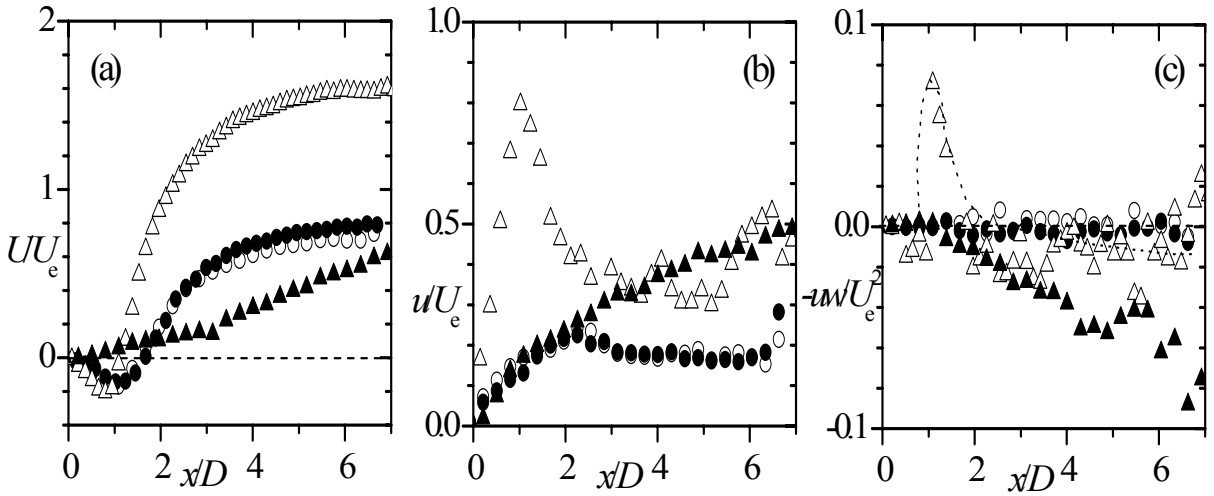

Fig. 5: Streamwise mean velocity distribution (a), turbulent intensity (b), and Reynolds shear stress along the wake axis for δ = 0.0° and 22.5°. Symbols: top cylinder (as in Figs. 3 and 4) δ = 0.0° (○), 22.5° (△); bottom cylinder (as in Figs. 3 and 4) δ = 0.0° (●), 22.5° (▲).

3.3.2. Mean velocity and turbulence intensities across wake

The profiles of streamwise mean velocity, turbulent intensities and Reynolds shear stress across the wakes at selected sreamwise locations (x/D = 2.5, 5.0, 7.5 and 10.0) are shown in Fig.6. In these plots, the spanwise distance (z) is normalized by the centre-centre spacing between the cylinder pairs (b = 51 mm). It should be noted that the profiles are staggered on the horizontal axis. At $\delta = 0°$, the mean velocity and turbulence intensity profiles are nearly symmetrical about the mid-plane between the cylinder pair ($z = 0$). As δ increases, the magnitude of the dimensionless mean velocity (U/U_e), turbulent intensities (u/U_e and w/U_e) and Reynolds shear stress ($-uw/U_e^2$) also increases. Moreover, the profiles of the mean velocity, turbulent intensities and Reynolds shear stress downstream of the inclined cylinders are asymmetric. At $\delta = 0°$, the profiles for the Reynolds shear stress are anti-symmetric.

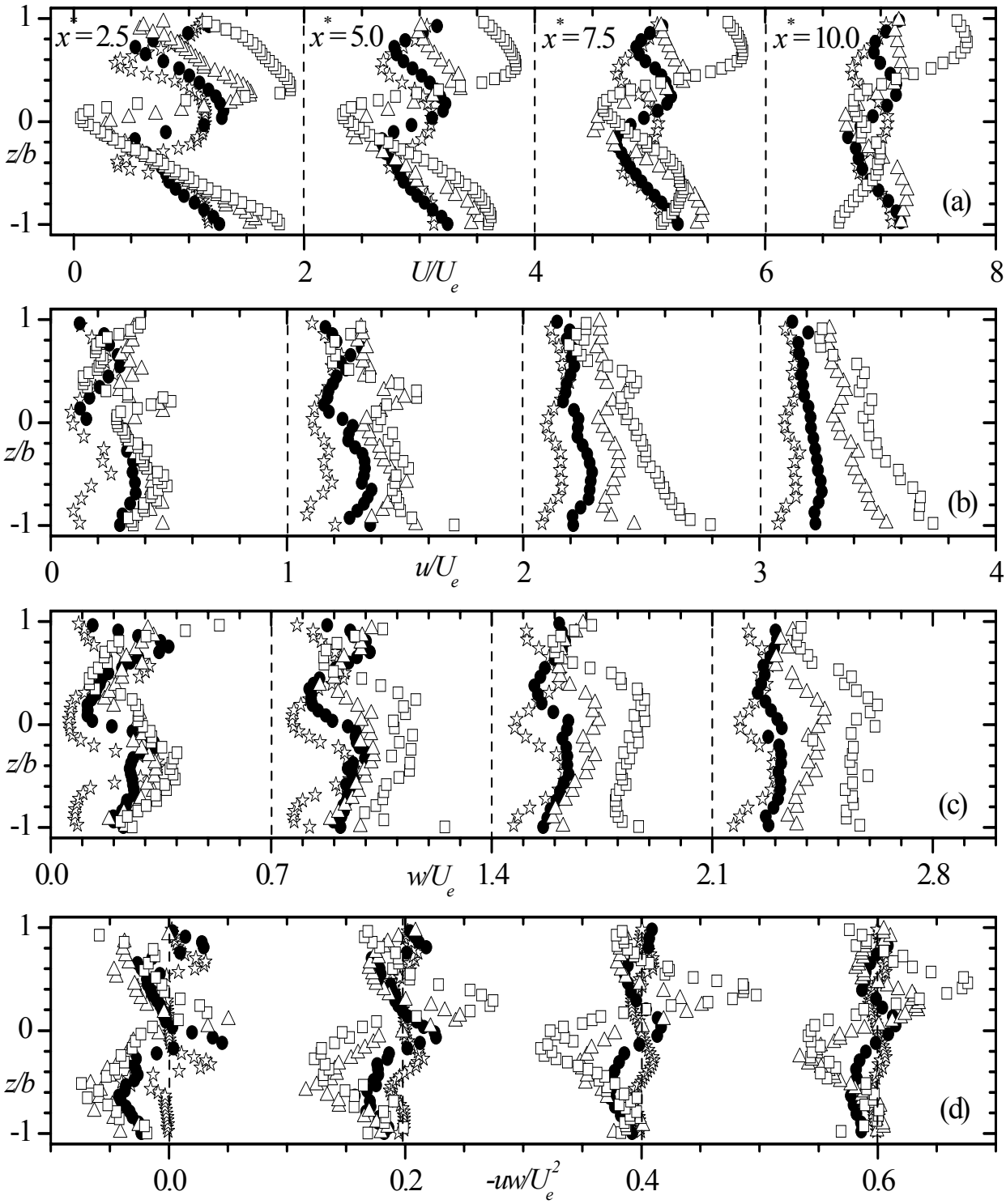

Fig. 6: Mean velocity and turbulent quantities at selected, $x^* = x/D$, locations (a) mean velocity, (b) streamwise , (c) spanwise turbulent intensities, and (d) Reynolds shear stress. Symbols: $\delta = 0.0°$ (☆), 7.5° (●), 15.0° (△), and 22.5° (□). All x^* locations correspond to those in (a).

4 CONCLUSIONS

The effects of cylinder inclination on the evolution of turbulent wakes of a pair of identical rectangular cylinders in an open channel have been investigated using a particle image velocimetry technique. It was found that the flow characteristics depend strongly on the cylinder inclination. When the inclination increased, strong asymmetric flow pattern was observed. The recirculation bubbles and the turbulence levels at the leeward side of inclined rectangular cylinders were larger than those at windward side. This has the implication of inducing asymmetric hydrodynamic loads that may lead to more severe vibration problems and ultimately to structure failure.

ACKNOWLEDGEMENTS

The authors acknowledge the financial support provided by Canada Foundation for Innovation, Natural Sciences and Engineering Research Council of Canada (Discovery Grant and CRD) and Manitoba Hydro.

REFERENCES

[1] Matsumoto, M. (1999), "Vortex Shedding of Bluff Bodies: a Review," *J. Fluid Structures*, **13**, 791 – 811.
[2] Knisley, C.W, (1990), "Strouhal Numbers of Rectangular Cylinders at Incidence: a Review and New Data," *J. Fluid Structures*, **4**, 371 – 393.
[3] Nakagawa, S., Nitta, K. and Senda, M. (1999), "An Experimental Study on Unsteady Turbulent near Wake of a Rectangular Cylinder in a Channel Flow," *Experiments in Fluids*, **27**(3), 284 - 294.
[4] Agelinchaab, M., Tsikata, J. M., Tachie, M. F. and Adane, K. K. (2008), "Turbulent Wake of Rectangular Cylinder Near Plane Wall and Free Surface," *AIAA Journal*, **46**(1), 104 - 117.
[5] Pal, S. (1985), "Freestream Turbulence Effects on Wake Properties of a Flat Plate at an Incidence," *AIAA Journal*, **23**, 1868 – 1871.
[6] Dutta, S., Muralidhar, K., and Panigrahi, P. K. (2003), "Influence of the orientation of a square cylinder on the wake properties," *Experiments in Fluids*, **34**, 16 – 23.
[7] van Oudheusden, B. W., Scarano, F., van Hinsberg, N. P. and Watt, D.W. (2005), "Phase-resolved characteristics of vortex shedding in the near wake of a square-section cylinder at incidence.'' *Experiments in Fluids*, **39**, 86 – 98.
[8] Raffel, M., Willert, C. E., and Kompenhaus, J., "Particle image velocimetry: A Practical Guide," Springer, 1998, New York, USA.
[9] Coleman, H. W. and Steele, W. G. (1995), "Engineering Application of Experimental Uncertainty Analysis," *AIAA Journal*, **33**(10), 1888 - 1896.
[10] Prasad, A. K., Adrian, R. J., Landreth, C. C., and Offutt, P.W. (1992), "Effect of resolution on the speed and accuracy of particle image velocimetry interrogation," *Experiments in Fluids*, **13**(2-3), 105 - 116.
[11] Forliti, D. J., Strykowski, P. J. and Debatin, K. (2000), "Bias and Precision Errors of Digital Particle Image Velocimetry," *Experiments in Fluids*, **28**(5), 436 - 447.